

1 **`Simple Tidy GeneCoEx`: a gene co-expression analysis workflow powered by tidyverse**
2 **and graph-based clustering in R**

3

4 Chenxin Li^{1*}, C. Robin Buell^{1,2,3}

5

6 ¹ Center for Applied Genetic Technologies, University of Georgia, Athens, GA, USA, 30602

7 ² Department of Crop and Soil Sciences, University of Georgia, Athens, GA, USA, 30602

8 ³ Institute of Plant Breeding, Genetics, and Genomics, University of Georgia, Athens, GA, USA,

9 30602

10

11 Received _____

12 * For correspondence: Chenxin.Li@uga.edu, Twitter: @ChenxinLi2

13

14 **Core Ideas**

- 15 • An R-based workflow that performs gene co-expression analysis was developed.
- 16 • The workflow is based on tidyverse packages and graph theory.
- 17 • The workflow is highly customizable, detects tight gene co-expression modules, and gen-
18 erates publication quality figures.
- 19 • Two plant gene expression datasets were used to benchmark the workflow.

20

21 **Abbreviations**

- 22 • ANCOVA: analysis of covariance
- 23 • ANOVA: analysis of variance

- 24 • FPKM: fragments per kilobase exon model per million mapped fragments
- 25 • LCM: laser capture micro-dissection
- 26 • msq: mean sum of squares
- 27 • PCA: principal component analysis
- 28 • sd: standard deviation
- 29 • TPM: transcripts per million
- 30 • WGCNA: weighted gene co-expression network analysis

31

32 **Abstract**

33 Gene co-expression analysis is an effective method to detect groups (or modules) of co-ex-
34 pressed genes that display similar expression patterns, which may function in the same biological
35 processes. Here, we present `Simple Tidy GeneCoEx`, a gene co-expression analysis workflow
36 written in the R programming language. The workflow is highly customizable across multiple
37 stages of the pipeline including gene selection, edge selection, clustering resolution, and data vis-
38 ualization. Powered by the tidyverse package ecosystem and network analysis functions provided
39 by the igraph package, the workflow detects gene co-expression modules whose members are
40 highly interconnected. Step-by-step instructions with two use case examples as well as source code
41 are available at https://github.com/cxli233/SimpleTidy_GeneCoEx.

42

43 **1. Introduction**

44 Transcriptomic analyses have become routine for studying plant biology. A challenge for plant
45 biologists is interpreting omics data to derive biological insights. A valuable and powerful tool for
46 gene expression analyses is gene co-expression. When multiple treatments (time points, develop-
47 mental stages, cell types, genotypes, and perturbations) are included in a gene expression study, it
48 is possible to detect groups of genes, or gene co-expression modules, with similar expression pro-
49 files across a range of treatment conditions or through a developmental timepoints. Under the
50 ‘guilt-by-association’ assumption, genes with expression patterns similar to previously character-
51 ized genes with known roles in a biological process (bait genes) are deduced to function in the
52 same biological process. In addition, candidate genes of interest can be detected in modules with
53 interesting expression patterns, which can then be subjected to further forward or reverse genetics
54 studies. Gene co-expression analyses have been successfully applied to identify genes implicated
55 in development, stress responses, primary metabolism, and specialized metabolism across a wide
56 range of plant species including crops and medicinal plants (Burlat et al. 2004; Anderson et al.
57 2017; Gomez-Cano et al. 2022; Moghaddam et al. 2021).

58 Due to its general ease of use, open-source nature, and availability of general and domain-
59 specific packages, the R programming language for statistical computing has become the program-
60 ming language of choice for gene expression and computational biology analyses (Tippmann
61 2015). Within the R programming environment, the tidyverse ecosystem is a collection of pack-
62 ages built upon a common programming style, grammar, and data structures (Wickham et al. 2019).
63 A key underlying concept of the tidyverse ecosystem is ‘tidy data frames’ which are data frames
64 with observations as rows and variables as columns. The ‘tidy’ nature of data frames greatly facil-
65 itates grouping, filtering, joining, reshaping, summarizing, and visualizing data using tidyverse

66 functions. Since gene expression matrixes are also tabular in nature, gene co-expression analyses
67 can be done in a tidyverse-compatible manner. Tidy data frames can be seamlessly integrated with
68 igraph (Csárdi and Nepusz 2006), a powerful network analysis package in R, as igraph contains
69 methods that converts data frames into network objects. In graph theory, a network is considered
70 a graph, a mathematical structure used to model pairwise relationships. Thus, the pairwise corre-
71 lations among genes can be modeled by a graph in which genes are nodes and correlations are
72 edges. Further, gene co-expression modules can be detected by graph-based clustering. Here, we
73 developed a gene co-expression workflow `Simple Tidy GeneCoEx` using tidyverse and igraph
74 functions. The workflow is highly customizable across multiple stages of the pipeline, including
75 gene selection, edge selection, clustering resolution, and data visualization. Step-by-step instruc-
76 tions for two benchmarked use cases are available at [https://github.com/cxli233/SimpleTidy_Gen-](https://github.com/cxli233/SimpleTidy_GeneCoEx)
77 [eCoEx](https://github.com/cxli233/SimpleTidy_GeneCoEx).

78

79 **2. Methods**

80 2.1 Overview

81 A straightforward pipeline was designed with plant molecular biologists and geneticists in mind:
82 (i) import gene expression matrix, (ii) filter for genes that are expressed, exhibit high variance,
83 and/or high F statistics, (iii) produce correlation matrix and filter edges, (iv) detect gene co-ex-
84 pression modules, and (v) plot/export results. The workflow is executed by calling tidyverse
85 (Wickham et al. 2019) and igraph (Csárdi and Nepusz 2006) functions.

86

87 2.2 Test Datasets

88 The workflow has been tested on two distinct datasets: tomato fruit developmental series (Shi-
89 nozaki et al. 2018) and tepary bean heat stress time course (Moghaddam et al. 2021). The tomato

90 fruit developmental series dataset contains six hand dissected tissues and five laser capture micro-
91 dissected (LCM) tissues across 11 developmental stages, ranging from anthesis to red ripe (i.e.,
92 fully ripe tomato fruits). For simplicity of demonstration, only hand dissected samples ($n = 84$
93 unique tissue by developmental stage combinations) were analyzed by this workflow, as it has
94 been noted that the LCM samples were lower input, constructed by a different library preparation
95 kit, and had globally distinct expression pattern relative to hand dissected samples (Shinozaki et
96 al. 2018). The tepary bean stress time course experiment contains two treatments (control vs. heat)
97 and five time points over a 24-hr period (1, 3, 6, 12, and 24 hours post stress), an experiment with
98 a strong diurnal component (Moghaddam et al. 2021). All treatment by time point combinations
99 ($n = 10$ combinations) were used in the test analyses. These datasets were chosen because of their
100 multifactorial experimental designs and distinct biological questions (development and stress) that
101 were investigated.

102 2.3 Required inputs

103 The workflow requires three inputs: (1) gene expression matrix, (2) library metadata, and (3)
104 bait genes. A variety of software can be used to generate gene expression matrices, such as Cuf-
105 flinks (Trapnell et al. 2012), kallisto (Bray et al. 2016), and STAR (Dobin et al. 2013). The required
106 format is that each row is a gene, and each column is a biological sample. Values in the gene co-
107 expression matrix should be depth and normalized gene expression estimates, in units of transcripts
108 per million (TPM) or fragments per kilobase of exon model per million mapped fragments (FPKM).
109 A metadata table is required for the workflow, in which each row corresponds to a sample (i.e.,
110 sequencing library), and columns correspond to biological and technical aspects of the libraries.
111 Finally, a table of bait genes is used to guide the pipeline, since oftentimes users have prior
112 knowledge of genes involved in the biological processes being studied. The required format is that

113 each row is a gene. Additional information about bait genes such as functional annotations and
114 genomic locations can be recorded as columns in the bait gene table. Before starting the workflow,
115 exploratory analyses, such as principal component analysis (PCA) are encouraged to examine the
116 major drivers of variance among samples.

117 2.4 Gene selection

118 Gene selection prior to co-expression analysis is optional. However, since the workflow con-
119 structs all pairwise correlations among genes, the number of correlations scales with the square of
120 number of genes in the analyses. Thus, pre-filtering genes can significantly speed up the workflow.
121 Gene selection can be performed using one or more of the following methods: expression threshold,
122 variance threshold, and F statistics threshold.

123 Gene selection based on expression value is the most conceptually simple. It asks if a given
124 gene is expressed among the samples being analyzed, given an expression threshold E and preva-
125 lence threshold N_P . A simple method is to subset genes with expression values $> E$ in at least N_P
126 libraries, where the values for E and N_P can be determined by the users based on the dataset. A
127 recommendation for selecting a prevalence threshold is to use the lowest level of replication across
128 treatments. For example, across all treatments in a study, if the treatment with the least number of
129 biological replicates has three replicates, then a recommended prevalence cutoff is $N_P = 3$.

130 More involved methods of gene selection are based on biological variance and F statistics. For
131 gene selection based on biological variances, the underlying assumption is that genes distinctly
132 expressed in one or more treatments have higher biological variances than genes expressed at sim-
133 ilar levels across all treatments. In this workflow, technical variation is reduced by first averaging
134 replicates to the level of the treatments. To reduce the bias towards highly expressed the genes,
135 pre-filtering high variance genes is done by first log-transforming the expression value, then

136 averaging replicates up to the level of treatments, and finally selecting high variance genes at the
137 log-transformed scale. Biological variance of bait genes can be used to determine the variance
138 threshold. For example, if user-selected bait genes are ranked among the highest 5000 variable
139 genes, then the top 5000 variable genes can be selected for downstream analyses (Fig. 1a, data
140 from (Shinozaki et al. 2018)).

141

142

143

144

145

146

147

148

149

150

151

152

153

154

155

156

157

158

159

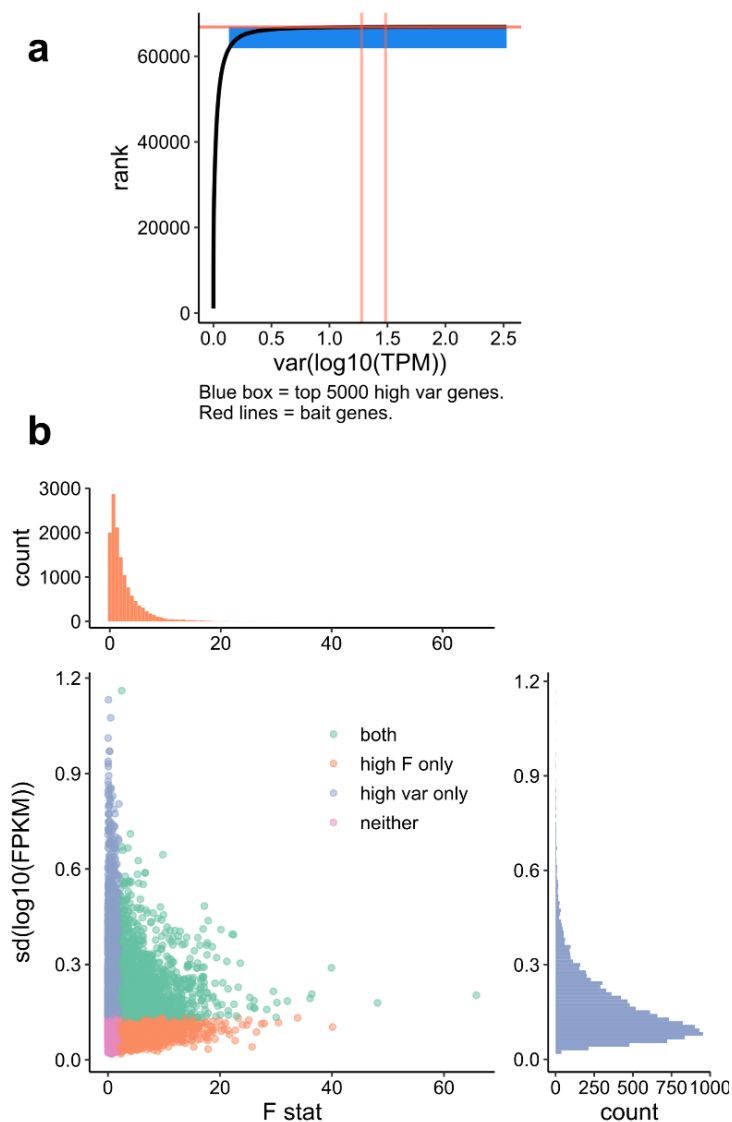


Fig. 1. Gene pre-filtering using biological variance and F statistics.

160
161 (a) Rank vs. value plot for transcripts (data from Shinozaki et al., 2018). Blue box includes top 5000 vari-
162 able genes, and orange lines correspond to two user-provided bait genes (Solly.M82.10G020850.1 and
163 Solly.M82.03G005440.1). In this analyses, the top 5000 variable transcripts were used for downstream
164 analyses.
165

166 (b) Scatter plot showing standard deviation (sd) and F statistics of expressed genes (data from Moghad-
167 dam et al. 2021). In this case, filtering for high variance or high F statistics ($F > 2$) do not select for the
168 same set of genes. In this analysis, the union of high variance and high F genes were used for downstream
169 analyses.
170

171 An alternative gene selection method to biological variance is the F statistics, which detects genes
172 whose expression levels are changing across treatments. The F statistics is computed by first fitting
173 a linear model for each gene:

$$\log(\text{expression}) \sim \text{treatment}$$

176
177 The dependent variable is log-transformed to reduce the heteroscedasticity and mean-error rela-
178 tionship associated with gene expression data. If the experiment is multifactorial in nature, then
179 users have the option to fit the linear model with the single factor accounting for the most varia-
180 tion in the dataset, or the interactions among two or more factors. Depending on the independent
181 variable(s) in the model, the F statistics reflect if a gene is changing expression across a single
182 factor or across the combinations of multiple factors. The F statistics are then calculated by
183 ANOVA. After the F statistics are computed for each gene, genes can be filtered by the F statis-
184 tics values. We discourage the use of p value for this gene selection method since most gene ex-
185 pression experiments have low levels of replication (typically $n = 3$). As a result, selecting F sta-
186 tistics using p value is overly conservative. Instead, we recommend an F statistics cutoff between
187 2 to 3. Depending on the model, high biological variance or high F statistics are not mutually ex-
188 clusive, nor do they select for the same set of genes (Fig. 1b, data from (Moghaddam et al.

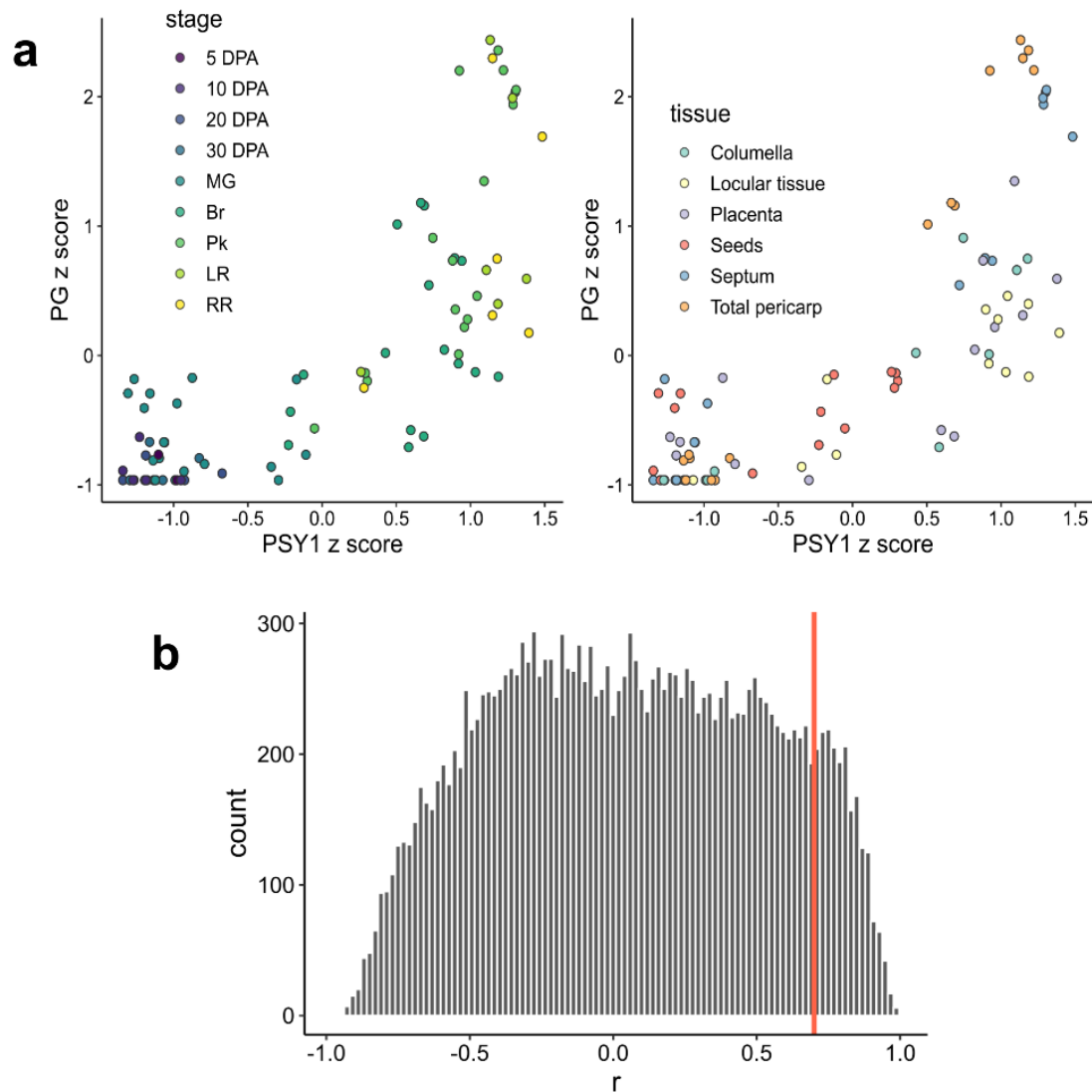
189 2021)). Depending on the biological questions of interest, high variance genes, high F statistics
190 genes, or the union can be used for downstream analyses.

191

192 2.5 Edge selection

193 Gene selection produces the nodes of the graph object for downstream network analyses. To
194 construct edges of the network, the workflow uses pairwise gene correlation on standardized log-
195 transformed expression values (z scores of log-transformed expression values). The correlation
196 matrix contains the Pearson correlation coefficient r of all pairwise correlations. A p value can be
197 computed from each correlation coefficient, which are then adjusted for multiple comparisons us-
198 ing the Benjamini-Hochberg procedure (Benjamini and Hochberg 1995). However, we encourage
199 users to derive an r cutoff based on empirical observations of bait genes instead of using adjusted
200 p values alone, since p value is affected by both r and degrees of freedom. Experiments with larger
201 number of treatments and thus higher degrees of freedom produce smaller p values given the same
202 r value. As a result, in experiments with large numbers of treatments, selecting an r cutoff based
203 solely on p values will be too non-stringent. Instead, prior knowledge regarding bait genes can be
204 used to guide edge selection. For example, users can examine the correlation between two bait
205 genes known to be co-expressed and select an r cutoff accordingly (Fig. 2, data from (Shinozaki
206 et al. 2018)). Alternatively, edge selection can be done using mutual ranks (Wisecaver et al. 2017;
207 Obayashi and Kinoshita 2009).

208



209

210 **Fig. 2. Edge selection using bait genes.**

211 (a) Scatter plots showing standardized z scores of *PSY1* and *PG*, two genes previously known to be co-
212 expressed (data from Shinozaki et al., 2018), $r = 0.75$. DPA: days post anthesis. MG: mature green. Br:
213 breaker. Pk: pink. LR: light red. RR: red ripe.

214
215 (b) Histogram showing distribution of correlation coefficient r . Based on correlation coefficient of known
216 co-expressed genes (shown in **a**), the cutoff is chosen at $r > 0.7$ (red line), beyond which the histogram
217 drops off rapidly.

218

219 2.6 Construction of the network object and graph-based clustering

220 The nodes (genes) and edges (correlations) are passed onto the ``graph_from_data_frame(``

221 function of `igraph` to generate the network object for graph-based clustering. Gene co-expression

222 modules are then detected using the Leiden algorithm (Traag, Waltman, and van Eck 2019), which

223 detects modules whose members are highly interconnected. The Leiden algorithm is implemented
224 using the `cluster_leiden()` function within the `igraph` package. A critical parameter for module
225 detection is resolution, which needs to be optimized for each experiment. Too low of a resolution
226 forces genes with different expression patterns into a single module, whereas too high of a resolu-
227 tion leads to many genes not contained in a module. The resolution parameter can be optimized by
228 testing a range of resolution values and monitoring the number of modules with 5 or more genes,
229 as well as the number of genes contained in modules with 5 or more genes. The minimum module
230 size 5 is chosen arbitrarily, but generally, higher resolution leads to more modules but less genes
231 contained in large modules (Fig 3).

232

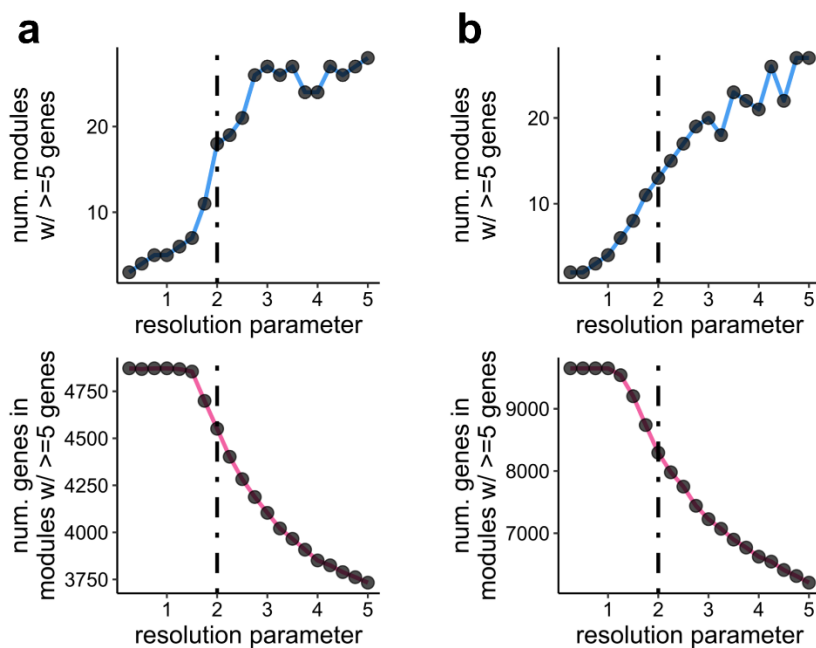


Fig. 3. Resolution for graph-based clustering

(a) Tradeoff between module number and genes retained (data from Shinozaki et al., 2018).

(b) Tradeoff between module number and genes retained (data from Moghaddam et al. 2021).

Dotted lines represent a resolution of 2, a compromise between the two performance indexes.

233

234 3. Results

235 3.1 Data visualization

236 From the gene co-expression modules detected by this workflow, a few data visualization op-
237 tions are available, such as heatmap and line graphs (Fig. 4). For heatmaps, the workflow reorders

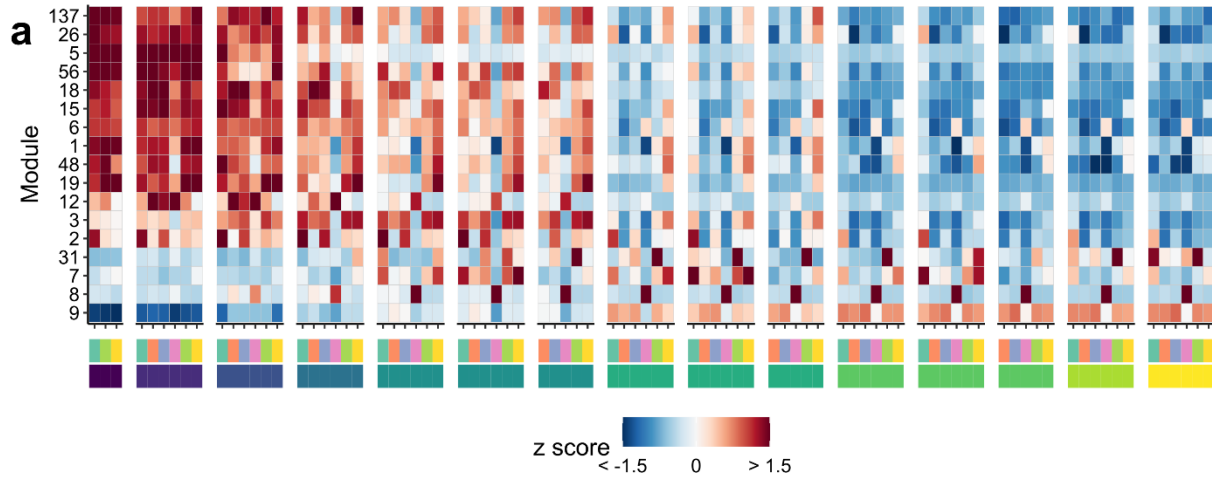
238 rows and columns based on module peak expression. The workflow was tested on two distinct use
239 cases: tomato fruit developmental series (Shinozaki et al. 2018) (Fig. 4a) and tepary bean heat
240 stress time course (Moghaddam et al. 2021) (Fig. 4b). The workflow can detect gene co-expression
241 modules that are highly expressed in early fruit development (e.g., Fig. 4a, Module 137) and fruit
242 ripening (Fig. 4a, Module 9), as well as tissue specific modules (Fig. 4a, Module 8, a seed specific
243 module). The workflow appears to perform well for experiments with a strong diurnal component,
244 as indicated by the detection of modules that appeared to cycle within a 24-hr period (Moghaddam
245 et al. 2021) (Fig. 4b, Module 7), in addition to stress-responsive modules (Fig. 4b, Modules 3 and
246 9). The workflow also provides methods for candidate gene identification using module member-
247 ship, as well as querying direct neighbors to bait genes using the ``neighbors()`` function within
248 igraph. Expression values of candidate genes (in the original scale or log-transformed scale) as
249 well as dispersion among replicates can be visualized (Fig. 4c).

250

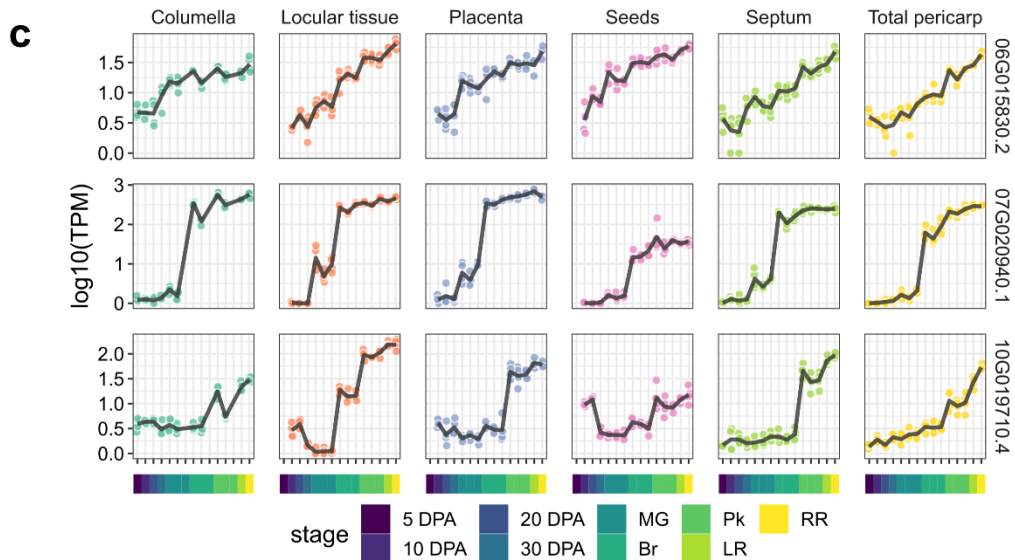
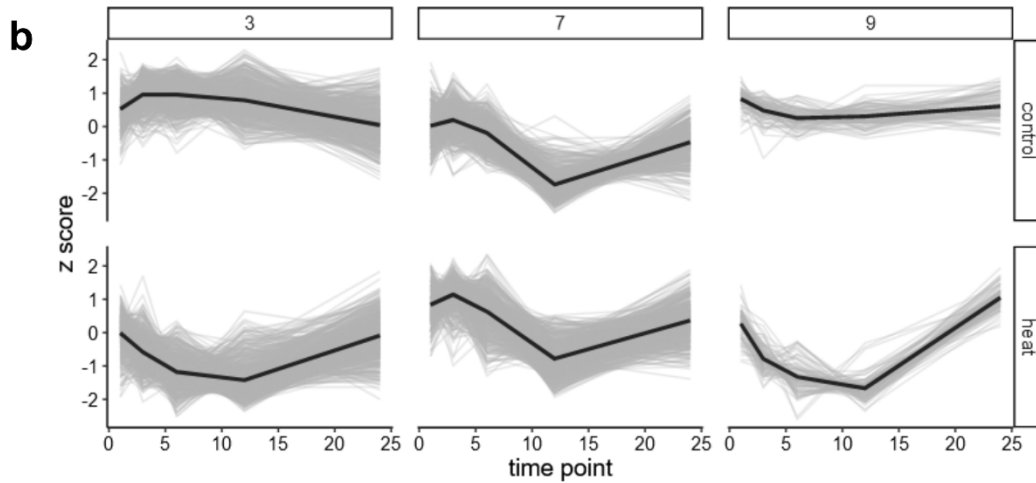
251 **Fig. 4. Heatmap and line graph visualization for gene co-expression modules.**

- 252
253 (a) Heatmap for gene co-expression modules (data from Shinozaki et al., 2018).
254 (b) Line graphs for gene co-expression modules (data from Moghaddam et al. 2021). Thin grey lines rep-
255 resent individual genes. Black lines represent the average expression pattern of the module.
256 (c) Line graphs showing exemplar candidate genes based on module membership (Module 9 in **a**) as well
257 as network neighborhood to bait genes (data from Shinozaki et al., 2018).

258

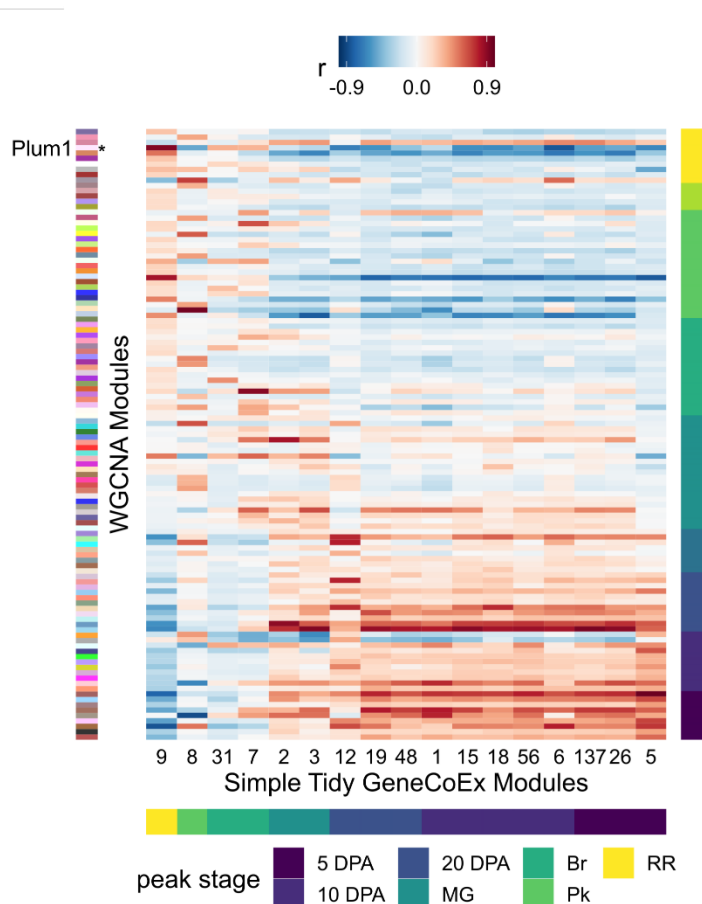


tissue Columella Locular tissue Placenta Seeds Septum Total pericarp
 stage 5 DPA 10 DPA 20 DPA 30 DPA MG Br Pk LR RR



260 3.2 Benchmarking against WGCNA

261 We benchmarked our `Simple Tidy GeneCoEx` method against Weighted Gene Coexpression
 262 Network Analysis (WGCNA), a widely accepted gene co-expression analysis package (Langfelder
 263 and Horvath 2008) using both use cases (tomato fruit development and tepary bean stress time
 264 course) (Shinozaki et al. 2018; Moghaddam et al. 2021). We found that both methods can detect
 265 treatment-specific/enriched gene co-expression modules. While there was a lack of a one-to-one
 266 correspondence between modules detected by the two methods, we detected groups of modules
 267 with similar expression patterns. For example, the “plum1” Module detected by WGCNA is highly
 268 correlated with Module 9 detected by this workflow; both peaked at the red ripe stage of tomato
 269 fruit development (Fig. 5). Analysis of module membership revealed the equivalence of a subset
 270 of modules detected by either method (Fig. 6). In some cases, the two methods detected modules

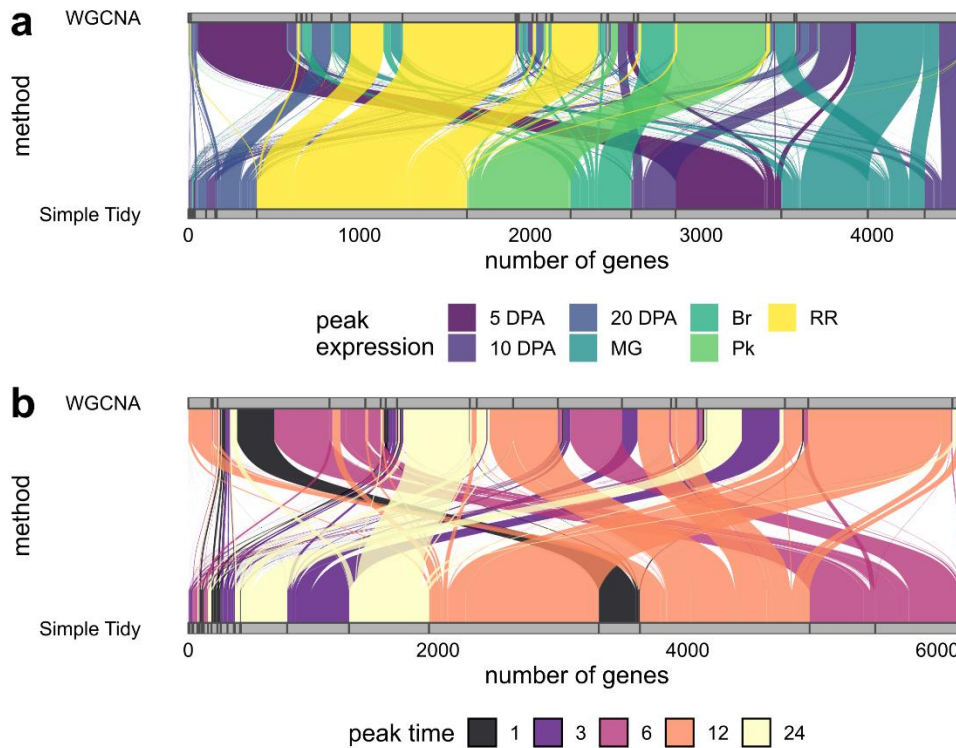


that share practically the same membership, while in other cases, a large module detected by one method is split into multiple smaller modules that have similar expression patterns by the other method.

Fig. 5. Module correspondence between WGCNA and `Simple Tidy Gene CoEx`.

Rows are gene co-expression modules detected by WGCNA, annotated by the color strip on the left. Columns are modules detected by `Simple Tidy GeneCoex`. Color strips at the bottom or on the right annotate the module peak

288 expression. Heatmap colors indicate correlation coefficient (r).
 289



290

291 **Fig. 6. Membership analyses between two gene co-expression methods, visualized by alluvial plots.**
 292 Horizontal grey bars represent gene co-expression modules. Blocks of colored curves represent shared
 293 membership.
 294

295 (a) data from Shinozaki et al. (2018).

296 (b) data from Moghaddam et al. (2021).

297

298 3.3 Module tightness

299 To evaluate and compare the quality or tightness of gene co-expression modules detected by
 300 either method, we computed the squared error loss for each module, which is defined as:

301

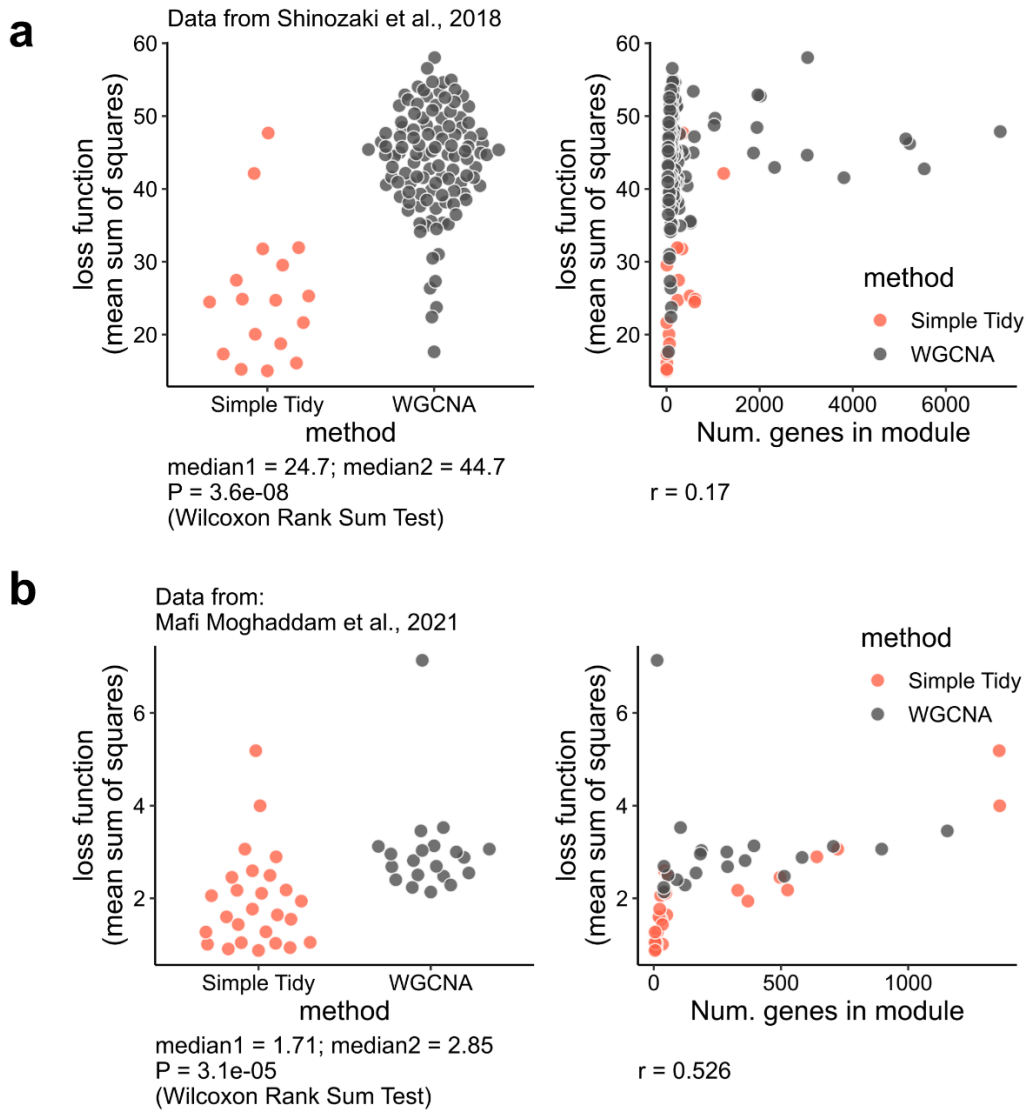
302 For gene i and treatment j in module m , the mean sum of square of such a module, i.e., msq_m , is
 303 computed by:

304

305
$$msq_m = \frac{\sum (z_{ijm} - \bar{z}_{jm})^2}{n_m}$$

306
307 where z_{ij} is the z score of each gene at each treatment, \bar{z}_{jm} is the average z score across all genes
308 in the module at each treatment, and n_m is the total number of genes in each module, such that the
309 sum of squares is normalized to the number of genes in each module.

310 We computed msq_m for each module detected by WGCNA or `Simple Tidy GeneCoEx` and
311 found that consistently for both use cases, the `Simple Tidy GeneCoEx` workflow detected mod-
312 ules with lower squared loss error (Fig. 7). For the Shinozaki et al. (2018) data, there was a ~45%
313 reduction in msq_m using `Simple Tidy GeneCoEx` relative to WGCNA ($P = 3.6 \times 10^{-8}$, Wilcoxon
314 Rank Sum Test). The association between msq_m and module size (number of genes in modules)
315 was weak ($r = 0.17$), suggesting the higher msq_m values for WGCNA modules is not due to insuf-
316 ficient clustering resolution (Fig. 7a). For data from Moghaddam et al. (2021) data, we saw a ~40%
317 reduction in msq_m using `Simple Tidy GeneCoEx` relative to WGCNA ($P = 3.1 \times 10^{-5}$, Wilcoxon
318 Rank Sum Test). We also observed a mild association between module size and msq_m ($r = 0.526$),
319 suggesting both methods may benefit from a higher clustering resolution (Fig. 7b). However, after
320 controlling for module size using a mixed effect linear model with module size as a random effect
321 covariate, on average, the `Simple Tidy GeneCoEx` workflow returned lower msq_m values (esti-
322 mate = -0.939, 95% confidence interval = [-1.6, -0.276], $F = 8.6$, $P = 0.0067$, ANCOVA). Taken
323 together, the `Simple Tidy GeneCoEx` workflow detects gene co-expression modules that are
324 tighter than those detected by WGCNA.



325

326 **Fig. 7. Quantification of module tightness.** Each data pot is a module, color coded by the gene co-ex-
327 pression method.
328

329 (a) data from Shinozaki et al. (2018).

330 (b) data from Moghaddam et al. (2021).

331

332 4. Discussion

333 Here, we present a simple, highly customizable co-expression analysis workflow in R powered

334 by tidyverse and igraph functions. The workflow has been tested on two distinct gene expression

335 studies (Shinozaki et al. 2018; Moghaddam et al. 2021), one focused on development and one

336 focused on a diurnal time course following heat stress. The workflow is applicable to other gene
337 expression studies such as single cell RNA-seq experiments. In a recent study, we applied this
338 workflow to detected co-expression modules enriched in specific cell types, which were used to
339 discover candidate genes in a biosynthetic pathway for complex plant natural products (Li et al.
340 2022). The method has been benchmarked against WGCNA, a widely accepted gene co-expression
341 package. We found that across two distinct use cases, the `Simple Tidy GeneCoEx` method detects
342 modules that are, on average, tighter than those detected by WGCNA. A potential reason underlying
343 the differences in module tightness might be due to the module detection methods. By default,
344 WGCNA uses hierarchical clustering followed by tree cutting to detect modules (Langfelder,
345 Zhang, and Horvath 2008). In contrast, `Simple Tidy GeneCoEx` uses the Leiden algorithm to
346 detect modules, which returns modules that are highly interconnected (Traag, Waltman, and van
347 Eck 2019).

348

349 **Data availability**

350 Gene expression matrix for Shinozaki et al. (2018) are available at Zenodo: [https://zenodo.org/rec-](https://zenodo.org/record/7117357)
351 [ord/7117357](https://zenodo.org/record/7117357). Gene expression matrix for Moghaddam et al. (2021) are available at GitHub:
352 https://github.com/cxli233/SimpleTidy_GeneCoEx/tree/main/Data/Moghaddam2022_data. Step-
353 by-step instructions for the workflow and source code are available at GitHub
354 https://github.com/cxli233/SimpleTidy_GeneCoEx, and stable release of source code are available
355 at Zenodo: <https://zenodo.org/record/7182680>.

356

357 **Conflict of Interest**

358 The authors declare no conflicts of interest.

359

360 **Author Contributions**

361 CL conceived the study, developed the pipeline, prepared figures, and wrote the manuscript with
362 input from CRB.

363

364 **Acknowledgements**

365 We thank Dr. Daniel Kliebenstein and John Hamilton for discussions regarding the pipeline. We
366 also thank Dr. Natalie Deans for producing the gene expression matrix from data published by
367 Shinozaki et al. (2018) using kallisto. We thank Drs. Mitchell Feldmann, Valerio Hoyos-Villegas,
368 Seth Murray, and Jason Wallace for discussions regarding mixed effect linear models. Funds from
369 the Georgia Research Alliance and the University of Georgia to CRB supported this work.

370

371 **Figure Legends**

372 **Fig. 1. Gene pre-filtering using biological variance and F statistics.**

373 (a) Rank vs. value plot for transcripts (data from Shinozaki et al., 2018). Blue box includes top
374 5000 variable genes, and orange lines correspond to two user-provided bait genes
375 (Solly.M82.10G020850.1 and

376 Solly.M82.03G005440.1). In this analyses, the top 5000 variable transcripts were used for down-
377 stream analyses.

378 (b) Scatter plot showing standard deviation (sd) and F statistics of expressed genes (data from
379 Moghaddam et al. 2021). In this case, filtering for high variance or high F statistics ($F > 2$) do
380 not select for the same set of genes. In this analysis, the union of high variance and high F genes
381 were used for downstream analyses.

382

383 **Fig. 2. Edge selection using bait genes.**

384 (a) Scatter plots showing standardized z scores of *PSYI* and *PG*, two genes previously known to
385 be co-expressed (data from Shinozaki et al., 2018), $r = 0.75$. DPA: days post anthesis. MG: ma-
386 ture green. Br: breaker. Pk: pink. LR: light red. RR: red ripe.

387 (b) Histogram showing distribution of correlation coefficient r . Based on correlation coefficient
388 of known co-expressed genes (shown in **a**), the cutoff is chosen at $r > 0.7$ (red line), beyond
389 which the histogram drops off rapidly.

390

391 **Fig. 3. Resolution for graph-based clustering**

392 (a) Tradeoff between module number and genes retained (data from Shinozaki et al., 2018).

393 (b) Tradeoff between module number and genes retained (data from Moghaddam et al. 2021).

394 Dotted lines represent a resolution of 2, a comprise between two the performance indexes.

395

396 **Fig. 4. Heatmap and line graph visualization for gene co-expression modules.**

397 (a) Heatmap for gene co-expression modules (data from Shinozaki et al., 2018).

398 (b) Line graphs for gene co-expression modules (data from Moghaddam et al. 2021). Thin grey
399 lines represent individual genes. Black lines represent the average expression pattern of the mod-
400 ule.

401 (c) Line graphs showing exemplar candidate genes based on module membership (Module 9 in
402 **a**) as well as network neighborhood to bait genes (data from Shinozaki et al., 2018).

403

404 **Fig. 5. Module correspondence between WGCNA and `Simple Tidy Gene CoEx`.**

405 Rows are gene co-expression modules detected by WGCNA, annotated by the color strip on the
406 left. Columns are modules detected by `Simple Tidy GeneCoex`. Color strips at the bottom or on
407 the right annotate the module peak expression. Heatmap colors indicate correlation coefficient
408 (r).

409

410 **Fig. 6. Membership analyses between two gene co-expression methods, visualized by allu-**
411 **vial plots.** Horizontal grey bars represent gene co-expression modules. Blocks of colored curves
412 represent shared membership.

413 (a) data from Shinozaki et al. (2018).

414 (b) data from Moghaddam et al. (2021).

415

416 **Fig. 7. Quantification of module tightness.** Each data pot is a module, color coded by the gene
417 co-expression method.

418 (a) data from Shinozaki et al. (2018).

419 (b) data from Moghaddam et al. (2021).

420

421 Reference

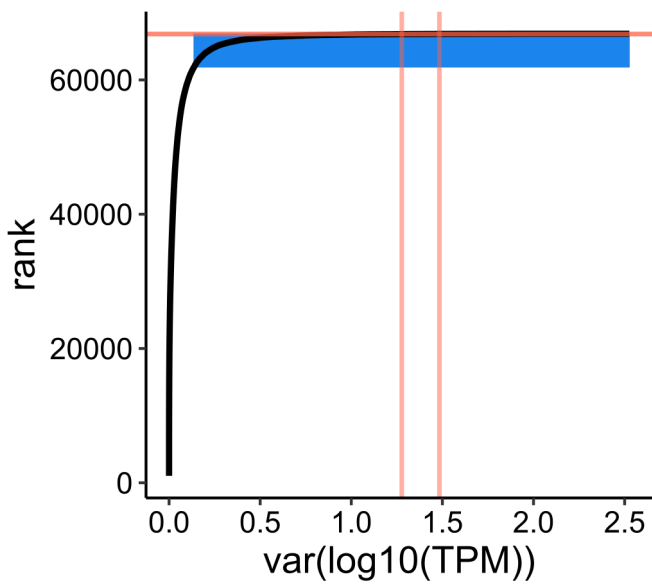
422 Anderson, Sarah N., Cameron S. Johnson, Joshua Chesnut, Daniel S. Jones, Imtiyaz Khanday,
423 Margaret Woodhouse, Chenxin Li, Liza J. Conrad, Scott D. Russell, and Venkatesan
424 Sundaresan. 2017. "The Zygotic Transition Is Initiated in Unicellular Plant Zygotes with
425 Asymmetric Activation of Parental Genomes." *Developmental Cell* 43 (3): 349-358.e4.
426 <https://doi.org/10.1016/j.devcel.2017.10.005>.

427 Benjamini, Yoav, and Yosef Hochberg. 1995. "Controlling the False Discovery Rate: A Practical
428 and Powerful Approach to Multiple Testing." *Journal of the Royal Statistical Society. Series B*
429 57 (1): 289-300.

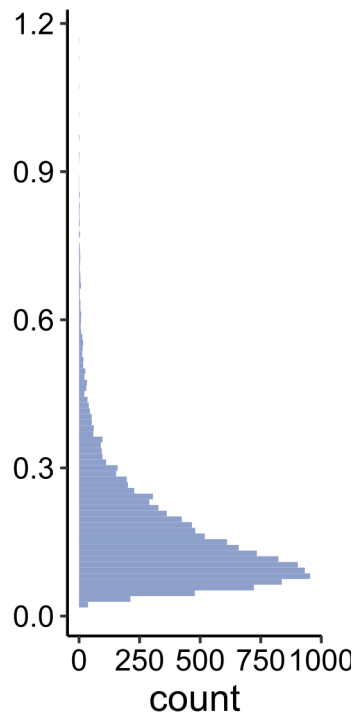
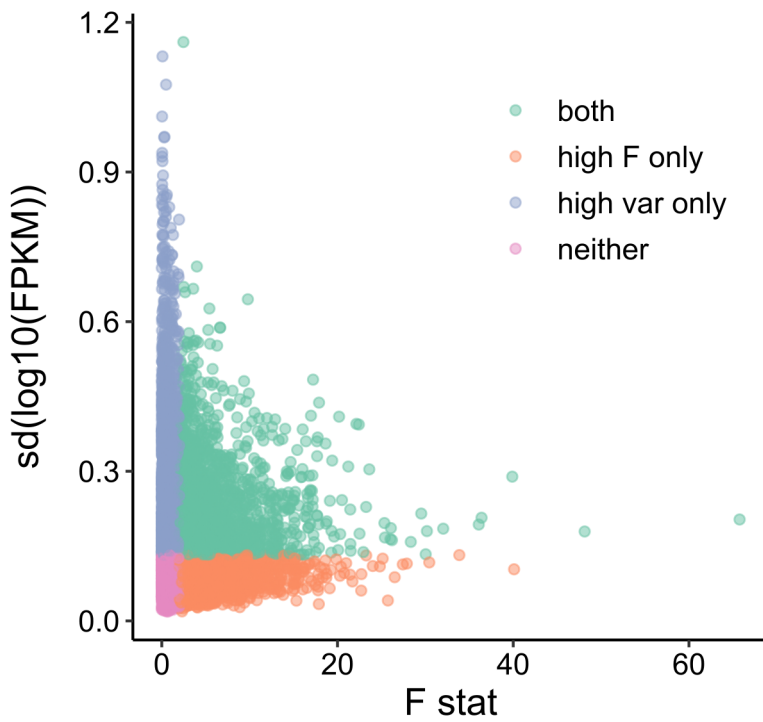
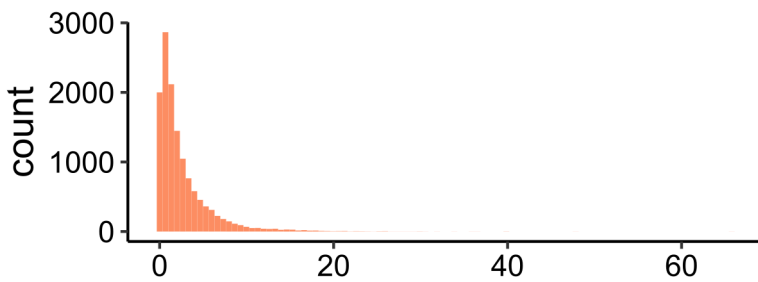
430 Bray, Nicolas L, Harold Pimentel, Páll Melsted, and Lior Pachter. 2016. "Near-Optimal Proba-
431 bilistic RNA-Seq Quantification." *Nature Biotechnology* 34 (5): 525-27.
432 <https://doi.org/10.1038/nbt.3519>.

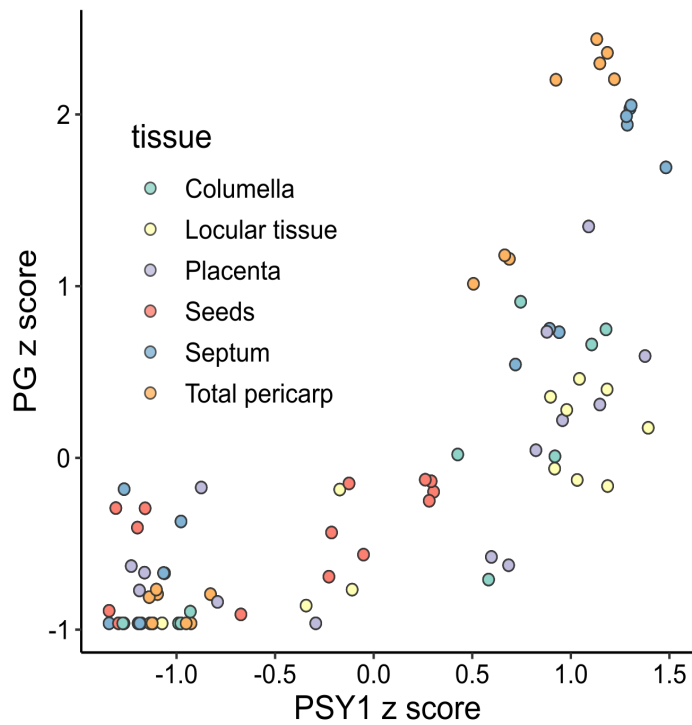
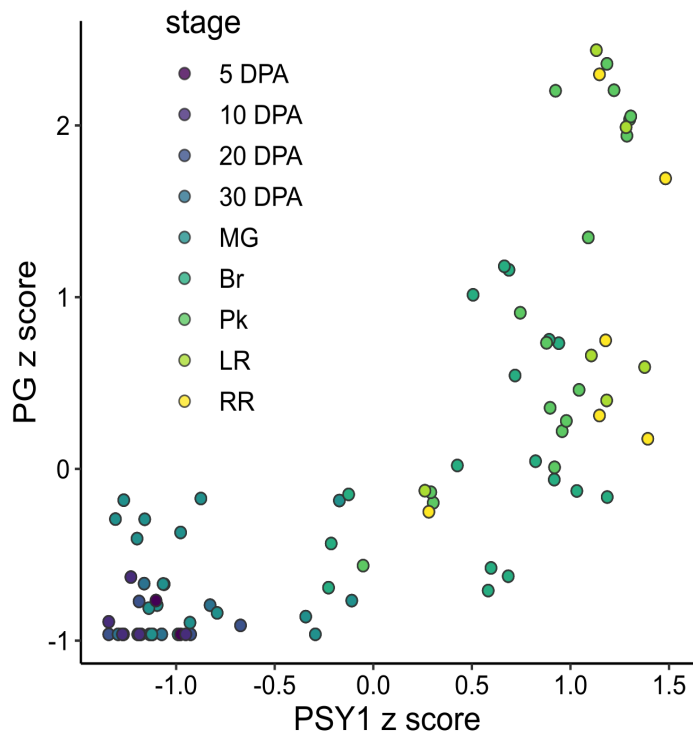
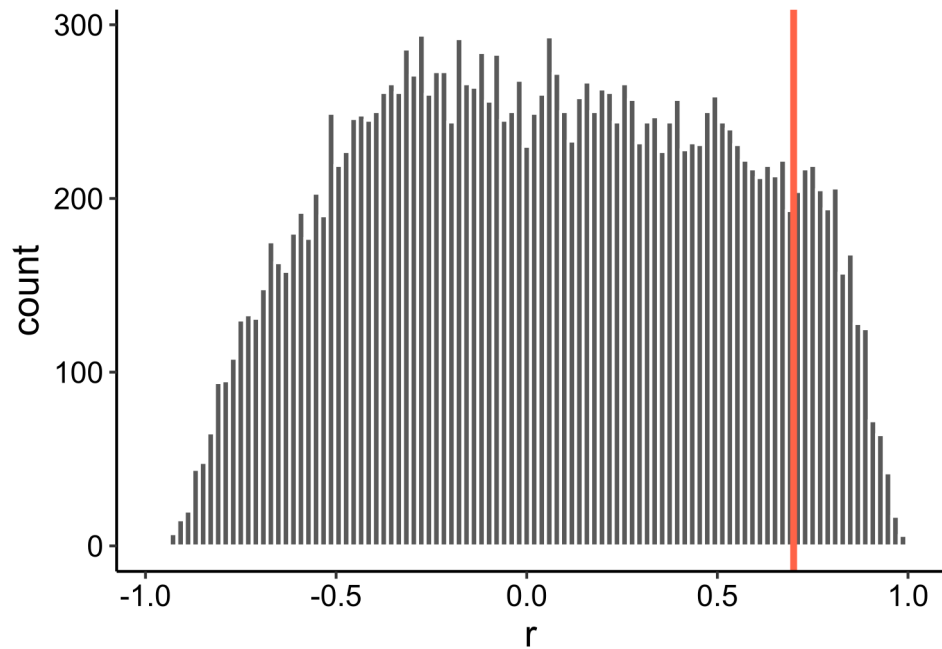
- 433 Burlat, Vincent, Audrey Oudin, Martine Courtois, Marc Rideau, and Benoit St-Pierre. 2004.
434 “Co-Expression of Three MEP Pathway Genes and *Geraniol 10-Hydroxylase* in Internal
435 Phloem Parenchyma of *Catharanthus Roseus* Implicates Multicellular Translocation of Inter-
436 mediates during the Biosynthesis of Monoterpene Indole Alkaloids and Isoprenoid-Derived
437 Primary Metabolites.” *The Plant Journal* 38 (1): 131–41. [https://doi.org/10.1111/j.1365-](https://doi.org/10.1111/j.1365-313X.2004.02030.x)
438 313X.2004.02030.x.
- 439 Csárdi, Gábor, and Tamás Nepusz. 2006. “The Igraph Software Package for Complex Network
440 Research.” *InterJournal, Complex Systems*, 1695. <https://igraph.org> .
- 441 Dobin, Alexander, Carrie A. Davis, Felix Schlesinger, Jorg Drenkow, Chris Zaleski, Sonali Jha,
442 Philippe Batut, Mark Chaisson, and Thomas R. Gingeras. 2013. “STAR: Ultrafast Universal
443 RNA-Seq Aligner.” *Bioinformatics* 29 (1): 15–21. [https://doi.org/10.1093/bioinformat-](https://doi.org/10.1093/bioinformatics/bts635)
444 ics/bts635.
- 445 Gomez-Cano, Fabio, Yi-Hsuan Chu, Mariel Cruz-Gomez, Hesham M. Abdullah, Yun Sun Lee,
446 Danny J. Schnell, and Erich Grotewold. 2022. “Exploring Camelina Sativa Lipid Metabolism
447 Regulation by Combining Gene Co-Expression and DNA Affinity Purification Analyses.” *The*
448 *Plant Journal* n/a (n/a). <https://doi.org/10.1111/tpj.15682>.
- 449 Langfelder, Peter, and Steve Horvath. 2008. “WGCNA: An R Package for Weighted Correlation
450 Network Analysis.” *BMC Bioinformatics* 9 (1): 559. [https://doi.org/10.1186/1471-2105-9-](https://doi.org/10.1186/1471-2105-9-559)
451 559.
- 452 Langfelder, Peter, Bin Zhang, and Steve Horvath. 2008. “Defining Clusters from a Hierarchical
453 Cluster Tree: The Dynamic Tree Cut Package for R.” *Bioinformatics* 24 (5): 719–20.
454 <https://doi.org/10.1093/bioinformatics/btm563>.
- 455 Li, Chenxin, Joshua C. Wood, Anh Hai Vu, John P. Hamilton, Carlos Eduardo Rodriguez Lopez,
456 Richard M. E. Payne, Delia Ayled Serna Guerrero, et al. 2022. “Single-Cell Multi-Omics Ena-
457 bled Discovery of Alkaloid Biosynthetic Pathway Genes in the Medical Plant *Catharanthus*
458 *Roseus*.” Preprint. *Plant Biology*. <https://doi.org/10.1101/2022.07.04.498697>.
- 459 Moghaddam, Samira Mafi, Atena Oladzad, Chushin Koh, Larissa Ramsay, John P. Hart, Sujan
460 Mamidi, Genevieve Hoopes, et al. 2021. “The Tepary Bean Genome Provides Insight into
461 Evolution and Domestication under Heat Stress.” *Nature Communications* 12 (1): 2638.
462 <https://doi.org/10.1038/s41467-021-22858-x>.
- 463 Obayashi, T., and K. Kinoshita. 2009. “Rank of Correlation Coefficient as a Comparable Meas-
464 ure for Biological Significance of Gene Coexpression.” *DNA Research* 16 (5): 249–60.
465 <https://doi.org/10.1093/dnares/dsp016>.
- 466 Shinozaki, Yoshihito, Philippe Nicolas, Noe Fernandez-Pozo, Qiyue Ma, Daniel J. Evanich,
467 Yanna Shi, Yimin Xu, et al. 2018. “High-Resolution Spatiotemporal Transcriptome Mapping
468 of Tomato Fruit Development and Ripening.” *Nature Communications* 9 (1): 364.
469 <https://doi.org/10.1038/s41467-017-02782-9>.
- 470 Tippmann, S. 2015. “Programming Tools: Adventures with R.” *Nature*, no. 517: 109–10.
471 <https://doi.org/doi:10.1038/517109a>.

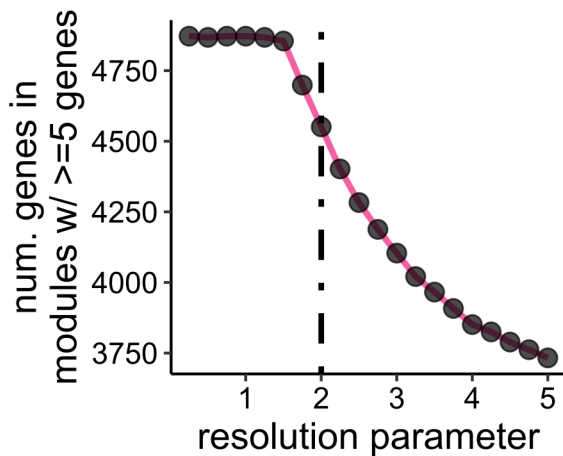
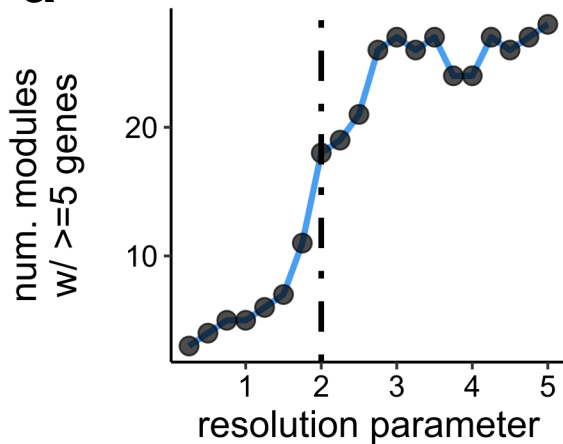
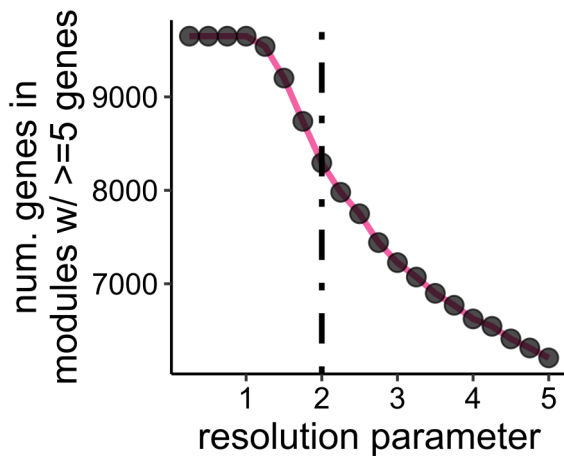
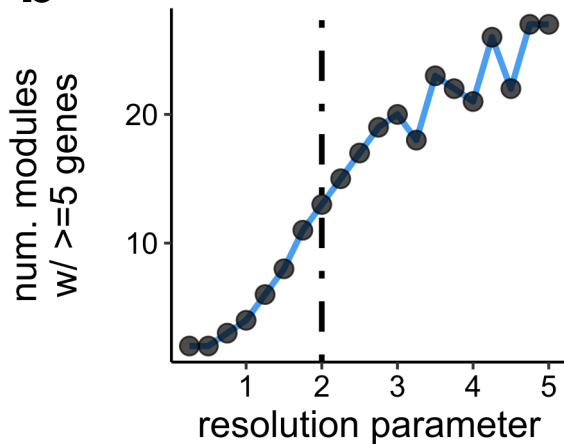
- 472 Traag, V. A., L. Waltman, and N. J. van Eck. 2019. “From Louvain to Leiden: Guaranteeing
473 Well-Connected Communities.” *Scientific Reports* 9 (1): 5233.
474 <https://doi.org/10.1038/s41598-019-41695-z>.
- 475 Trapnell, Cole, Adam Roberts, Loyal Goff, Geo Pertea, Daehwan Kim, David R Kelley, Harold
476 Pimentel, Steven L Salzberg, John L Rinn, and Lior Pachter. 2012. “Differential Gene and
477 Transcript Expression Analysis of RNA-Seq Experiments with TopHat and Cufflinks.” *Nature
478 Protocols* 7 (3): 562–78. <https://doi.org/10.1038/nprot.2012.016>.
- 479 Wickham, Hadley, Mara Averick, Jennifer Bryan, Winston Chang, Lucy McGowan, Romain
480 François, Garrett Grolemond, et al. 2019. “Welcome to the Tidyverse.” *Journal of Open
481 Source Software* 4 (43): 1686. <https://doi.org/10.21105/joss.01686>.
- 482 Wisecaver, Jennifer H., Alexander T. Borowsky, Vered Tzin, Georg Jander, Daniel J. Klie-
483 benstein, and Antonis Rokas. 2017. “A Global Coexpression Network Approach for Connect-
484 ing Genes to Specialized Metabolic Pathways in Plants.” *The Plant Cell* 29 (5): 944–59.
485 <https://doi.org/10.1105/tpc.17.00009>.
- 486

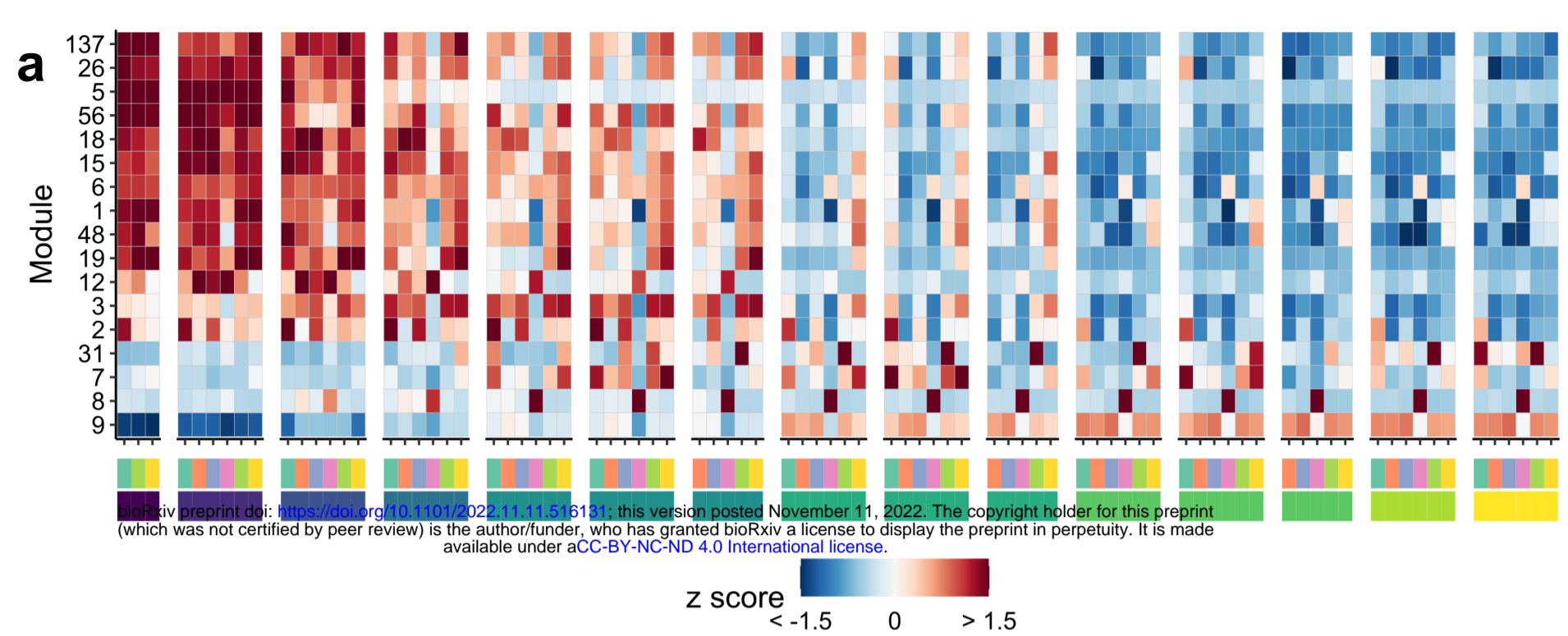
a

Blue box = top 5000 high var genes.
Red lines = bait genes.

b

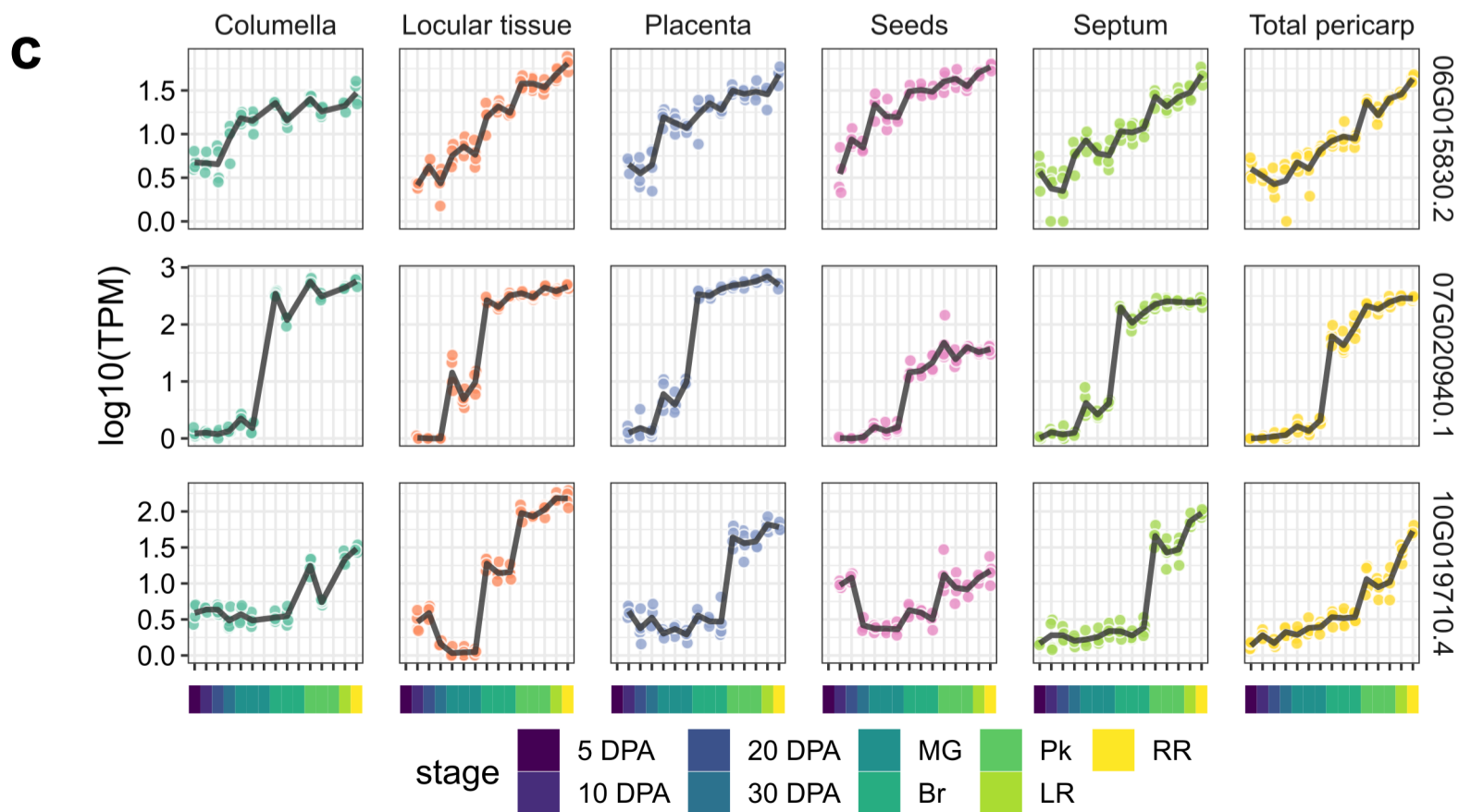
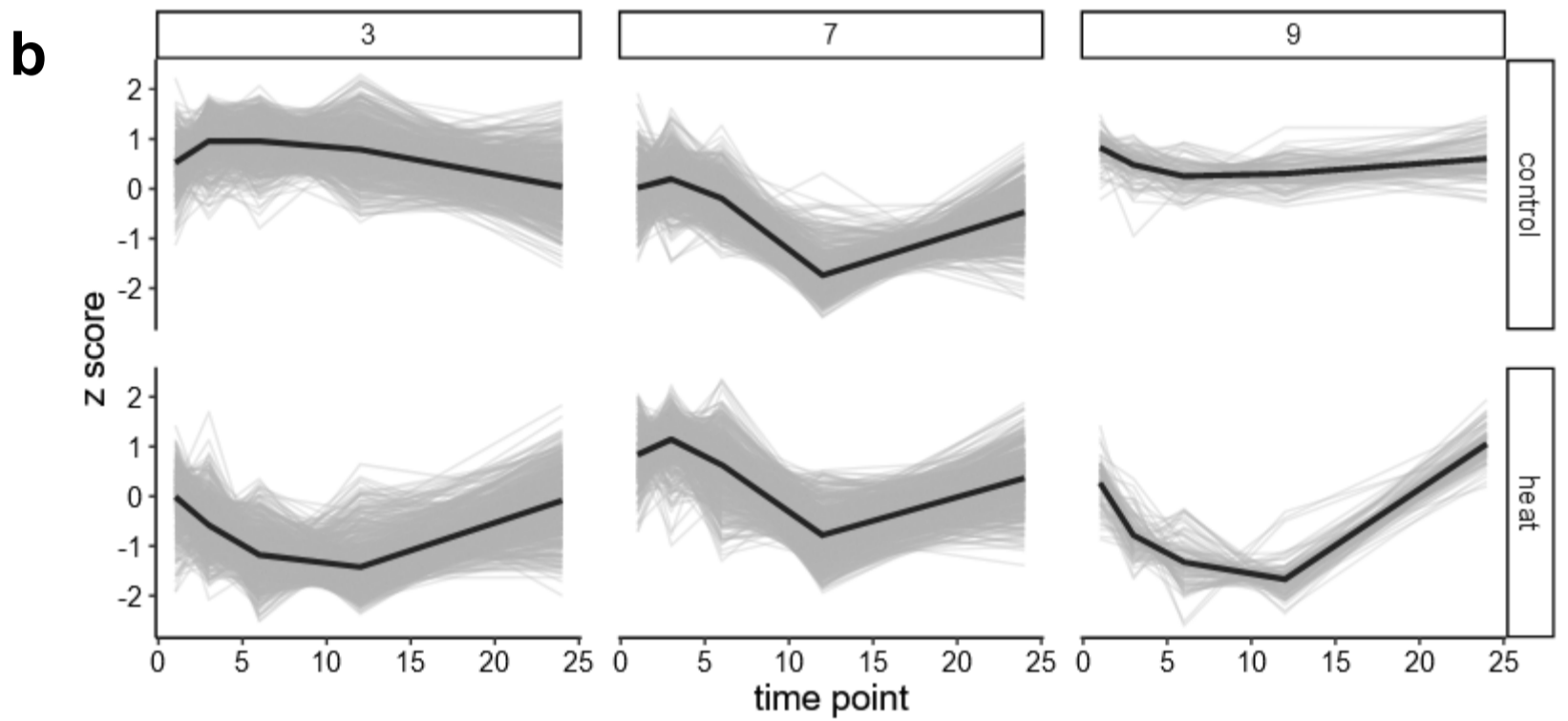
a**b**

a**b**



tissue ■ Columella ■ Locular tissue ■ Placenta ■ Seeds ■ Septum ■ Total pericarp

stage ■ 5 DPA ■ 10 DPA ■ 20 DPA ■ 30 DPA ■ MG ■ Br ■ Pk ■ LR ■ RR

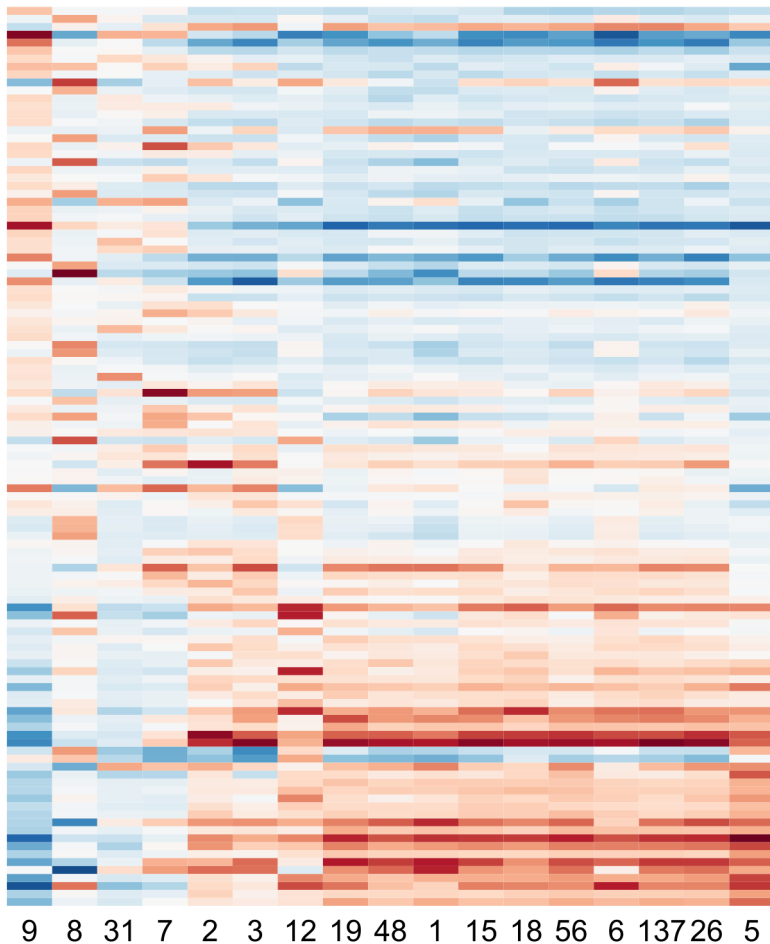




Plum1 *



WGCNA Modules



9 8 31 7 2 3 12 19 48 1 15 18 56 6 137 26 5

Simple Tidy GeneCoEx Modules



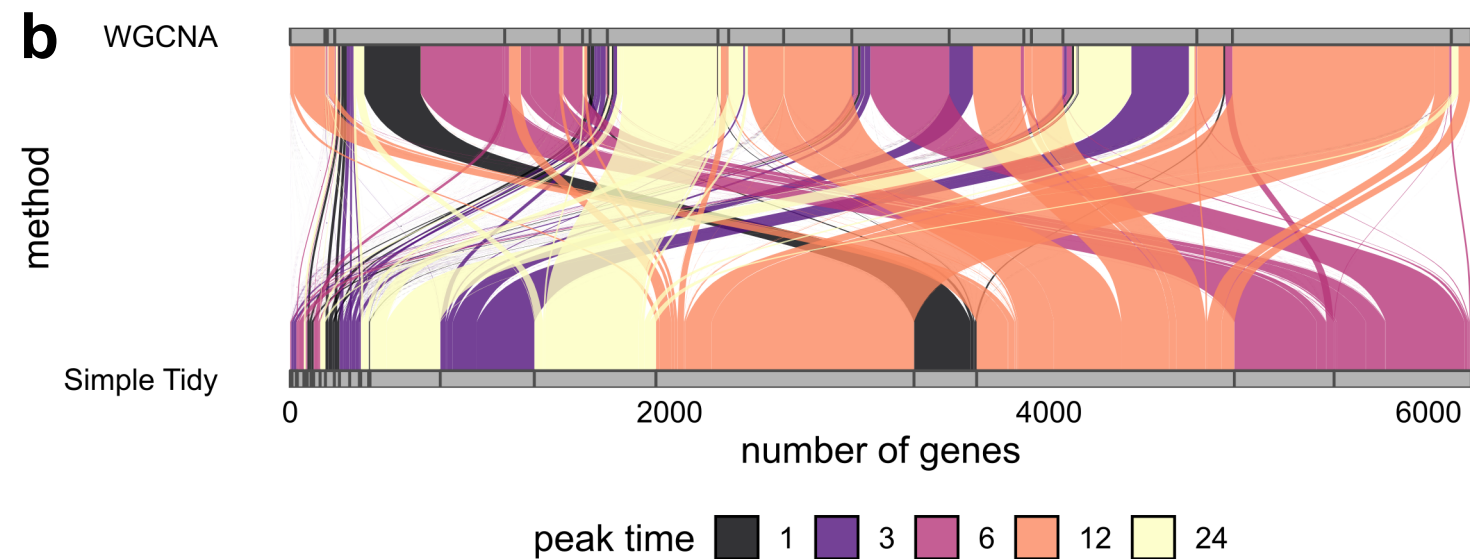
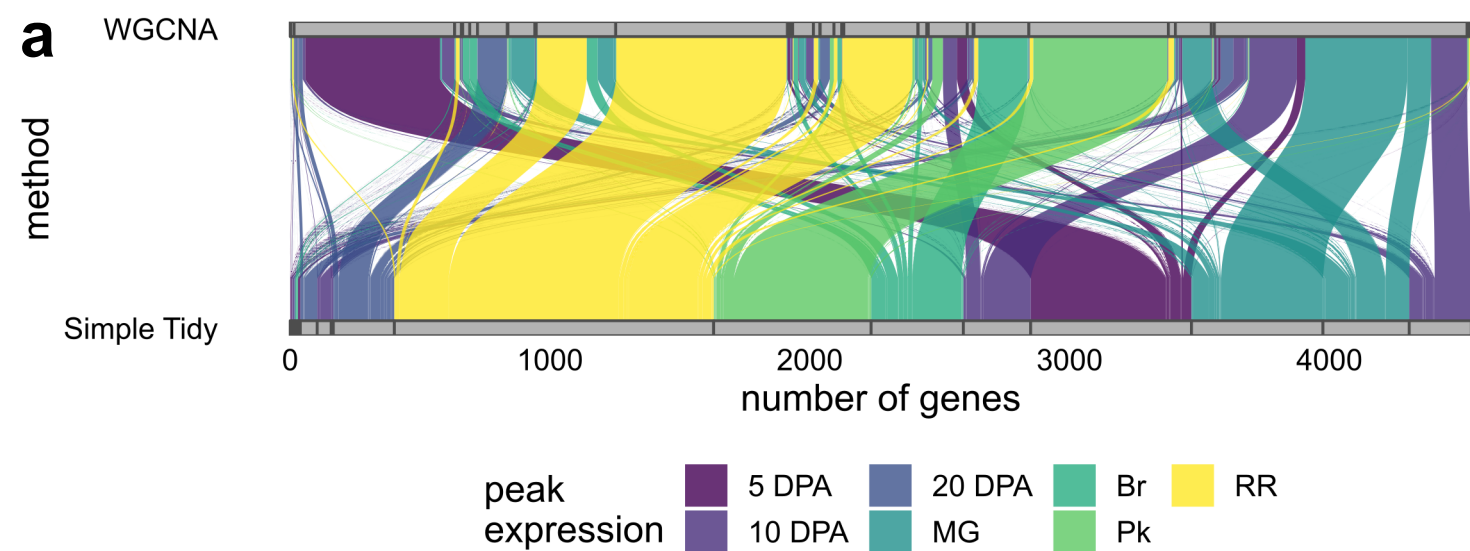
peak stage

5 DPA
10 DPA

20 DPA
MG

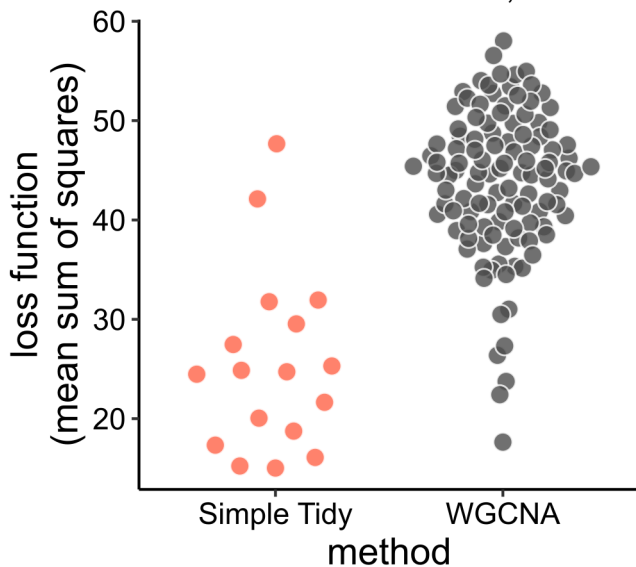
Br
Pk

RR

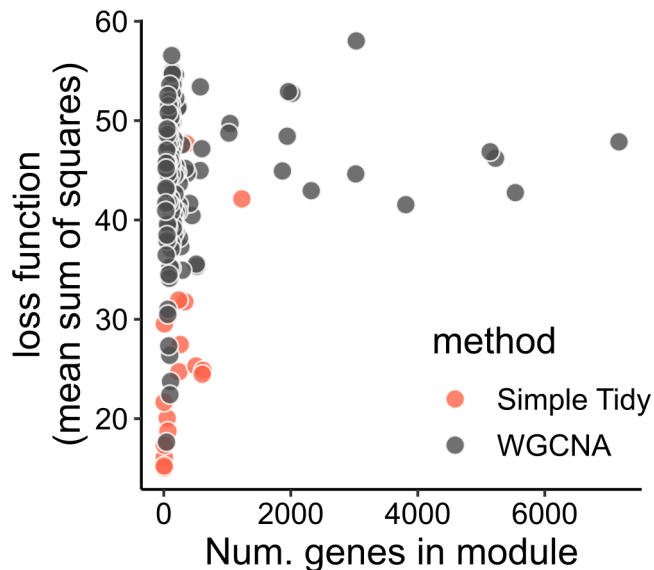


a

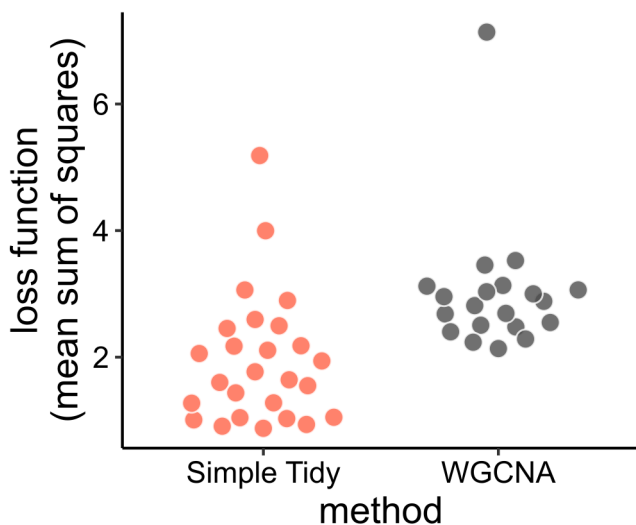
Data from Shinozaki et al., 2018



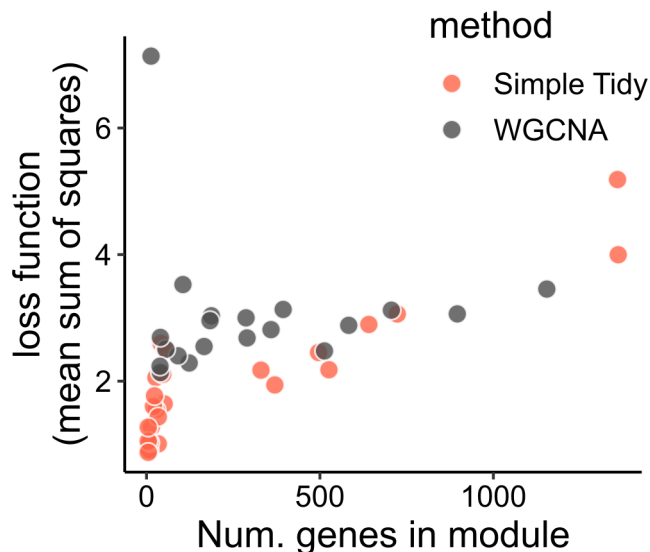
median1 = 24.7; median2 = 44.7
 P = 3.6e-08
 (Wilcoxon Rank Sum Test)



$r = 0.17$

bData from:
Mafi Moghaddam et al., 2021

median1 = 1.71; median2 = 2.85
 P = 3.1e-05
 (Wilcoxon Rank Sum Test)



$r = 0.526$